

Effect of different iodide salts on ionic conductivity and structural and thermal behavior of rice-starch-based polymer electrolytes for dye-sensitized solar cell application

M. H. Khanmirzaei · S. Ramesh · K. Ramesh

Received: 29 November 2014 / Revised: 23 January 2015 / Accepted: 2 February 2015 / Published online: 13 February 2015
© Springer-Verlag Berlin Heidelberg 2015

Abstract Biodegradable-based rice starch is used to prepare polymer electrolytes (PEs) using different iodide salts. Lithium iodide (LiI), ammonium iodide (NH₄I), and sodium iodide (NaI) are used in this work. Polymer electrolytes are prepared using solution cast technique. The ionic conductivity of PEs is measured and temperature-dependent behavior of PEs studied. The polymer electrolyte system containing sodium iodide shows the highest ionic conductivity upon addition of 45 wt% sodium iodide. Fourier transform infrared (FTIR) results confirm complexation between polymer and salt. Thermal behavior of PEs is studied under thermogravimetric analysis (TGA) and differential scanning calorimetry (DSC). The polymer electrolyte with 45 wt% of NaI is used to fabricate dye-sensitized solar cell (DSSC) and analyzed under Sun simulator. It shows short-circuit current density (mA cm⁻²), open circuit voltage (mV), and fill factor (%) of 2.40, 0.485, and 67.0, respectively.

Keywords Rice starch · Polymer electrolyte · Lithium iodide · Ammonium iodide · Sodium iodide · DSSC

Introduction

Biodegradable polymers have various advantages such as low cost, being environmentally friendly, nontoxic, and available abundantly in nature. Due to these advantages, biodegradable-

based polymer electrolytes have been significantly studied for electrochemical applications such as dye-sensitized solar cells [1, 2], batteries [3–6], super capacitors [7–9], fuel cells [10, 11], and electrochromic devices [12]. Among the biodegradable polymers, starch as natural polymer is widely investigated as biodegradable-based polymer electrolytes and in electrochemical applications [13–15].

Rice starch is a good candidate among other starches because rice starch has high amylose and low viscosity [16]. As 1,4- α linkages in amylose are more stable and less steric than 1,6- α linkages, the mobile ions after addition of salt attach more on the amylose units. Thus, rice starches with high amylose content are expected to have more mobile ions and higher ionic conductivity [17].

In this work, polymer electrolytes based on rice starch incorporated with lithium iodide, ammonium iodide, and sodium iodide were prepared. The effect of iodide salts on conductivity and structural and thermal properties were studied using electrochemical impedance spectroscopy (EIS), Fourier transform infrared (FTIR), thermogravimetric analysis (TGA), and differential scanning calorimetry (DSC). Polymer-electrolyte-based dye-sensitized solar cell was fabricated using the polymer electrolyte with the highest ionic conductivity.

Experimental

Materials

Biodegradable rice starch (RS) purchased from Sigma-Aldrich was used without further purification. Lithium iodide salt (LiI) was purchased from Aldrich (crystalline powder, 99.9 % trace metals basis). Ammonium iodide (NH₄I) and sodium iodide (NaI) were purchased from Sigma-Aldrich

M. H. Khanmirzaei · S. Ramesh (✉) · K. Ramesh
Centre for Ionics University of Malaya, Department of Physics,
Faculty of Science, University of Malaya, 50603 Kuala
Lumpur, Malaysia
e-mail: rameshtsubra@gmail.com

M. H. Khanmirzaei
e-mail: mhassan1358@hotmail.com

(assay $\geq 99\%$). The iodide salts were kept dry before use. TiO₂ P90 (14 nm) and P25 (21 nm) were purchased from Aeroxide. Triton X-100 was purchased from Sigma-Aldrich and Carbowax from Supelco Analytical.

Polymer electrolyte preparation

Polymer electrolytes were prepared using solvent cast method. Three different systems with rice starch incorporating LiI, NH₄I, and NaI were performed. All the systems follow the equation: RS+Xwt% Y (X=5, 10, 15, 20, 25, 30, 35, 40, 45; Y=LiI, NH₄I, and NaI). The system with LiI was designated as system S1, NH₄I as system S2, and NaI as system S3, which is expressed in Table 1. For each sample, 25 ml of distilled water was used as solvent. Appropriate amounts of rice starch were added into distilled water and heated until 80 °C for about 15 min to dissolve and gelatinize the rice starch. After gelatinization of the rice starch, appropriate amounts of iodide salt (NH₄I and NaI) were added according to Table 1. The mixtures were stirred to obtain a homogeneous solution and cast onto Teflon Petri dishes. Subsequently, any amounts of water were evaporated in a drying oven at 60 °C for 24 h. After drying, the solid polymer electrolytes were cast and analyzed directly at room temperature. The system preparation containing LiI was performed in our previous work [17].

Dye-sensitized solar cell fabrication

Photo-electrode layer was prepared with two TiO₂ layers on the fluorine-doped tin oxide (FTO) substrate. For the first layer, which was spin-coated, 0.5 g of TiO₂ (P90) was grounded for 30 min with 2 ml HNO₃ (pH=1) in an agate mortar and spin coated on FTO at 1000 rpm for 2 s and after with 2350 rpm for 60 s, and finally sintered at 450 °C for 30 min. For the second layer, 0.5 g of TiO₂ (P25) was grounded for

30 min with 2 ml HNO₃ (pH=1) in agate mortar with one drop of Triton X-100 and 0.1 g Carbowax; and later, the solution was doctor-bladed on the first layer and sintered at 450 °C for 30 min. Later, this electrode was soaked in N719 dye solution for 24 h. Counter electrode was prepared using commercial platinum solution and coated on FTO substrate and then sintered at 450 °C for 30 min. The prepared polymer electrolyte with the highest ionic conductivity was sandwiched between two electrodes and analyzed under Sun simulator.

Characterization methods

For ionic conductivity and temperature-dependent conductivity study, the samples were studied using EIS, Hioki, 3532-50 LCR HiTESTER. Structural properties were analyzed using FTIR spectrometer (Thermo Scientific, Nicolet iS10). The wavenumbers region was between 4000 and 400 cm⁻¹ with 2 cm⁻¹ resolution. Nitrogen gas was used to blank FTIR in order to remove CO₂ and water from the environment. Infrared spectra of samples were collected after background collection. X-ray diffraction (XRD) patterns of samples were recorded using XRD Siemens D 5000 diffractometer (40 kV, 40 mA) with Cu K α radiation and wavelength of $\lambda = 1.540600 \text{ \AA}$ for 2θ range of 5–80° at ambient temperature. TGA was carried out using TA Instrument Universal Analyzer TGA Q500. Nitrogen flow rate for balance gas and sample gas were 40 and 60 ml/min, respectively. The samples were heated with ramping rate of 50 °C/min from 4 to 700 °C to obtain decomposition temperature (T_{dc}). DSC analysis was performed on the polymer electrolyte using TA Instrument Universal Analyzer DSC Q2000 with refrigerated cooling system (RCS90). The experiment was performed under nitrogen flow rate of 50 ml/min. Samples were in the range of 3–5 mg and sealed in the Tzero aluminum hermetic pan. The samples were analyzed in heat-cool-heat process within 4 cycles with heating and cooling rate of 10 °C/min. At the first, the system

Table 1 Designation and ionic conductivity of three polymer electrolyte systems (S1, S2, and S3)

Designation			RS:X (wt-%) composition (X=LiI, NH ₄ I, NaI)	Conductivity, σ (S cm ⁻¹)		
S1	S2	S3		S1	S2	S3
RS-0	–	–	100:0	6.87×10^{-10}	–	–
RS-1	RN-1	RNa-1	95:5	1.87×10^{-8}	1.02×10^{-9}	3.32×10^{-9}
RS-2	RN-2	RNa-2	90:10	3.33×10^{-8}	1.13×10^{-9}	9.03×10^{-9}
RS-3	RN-3	RNa-3	85:15	1.66×10^{-8}	1.22×10^{-9}	4.56×10^{-8}
RS-4	RN-4	RNa-4	80:20	1.59×10^{-7}	1.32×10^{-8}	1.55×10^{-7}
RS-5	RN-5	RNa-5	75:25	2.47×10^{-6}	1.58×10^{-6}	3.03×10^{-8}
RS-6	RN-6	RNa-6	70:30	3.83×10^{-6}	2.18×10^{-5}	3.05×10^{-7}
RS-7	RN-7	RNa-7	65:35	4.68×10^{-5}	2.22×10^{-5}	1.40×10^{-5}
RS-8	RN-8	RNa-8	60:40	–	3.68×10^{-5}	5.22×10^{-5}
RS-9	RN-9	RNa-9	55:45	–	1.39×10^{-4}	4.79×10^{-4}

was equilibrated at 105 °C for 2 min for isothermal purposes and equilibrated at −90 °C for cycle 1. In cycle 2, the rate of 20 °C/min was applied to 230 °C. In cycle 3, this procedure was applied to −80 °C from the previous cycle. Finally, in cycle 4, this process was applied to 230 °C. Cycle 4 was used to calculate glass transition temperature (T_g).

Results and discussion

Electrochemical impedance spectroscopy

Ionic conductivity

Polymer electrolytes for all three systems were analyzed using EIS. Ionic conductivity was measured for all samples. Figure 1 shows variation of the ionic conductivity with different iodide salt content. The highest ionic conductivities achieved for systems S1, S2, and S3 are 4.68×10^{-5} , 1.39×10^{-4} , and 4.79×10^{-4} S/cm, respectively. The highest ionic conductivity between three systems is in system S3 after incorporation of 45 wt% NaI (RNa-9). Table 1 shows designation and measured ionic conductivity of all systems. The results show that the ionic conductivity increases after addition of iodide salt. This is due to increase in mobile ions of iodide salts incorporated in systems. On the other hand, the mobile ions can enhance the electrical performance in the system [18]. Table 2 demonstrates bulk resistance (R_b) of three systems as impedance data. The results in Table 2 show the R_b decrease with the addition of iodide salts, which reach minimum value in RNa-9.

Furthermore, the NaI salt shows more ionic conductivity enhancement compare to LiI and NH_4I salt, which may be related to higher mass in sodium as ionic carrier according to Rice and Roth model [19] expressed as below equation

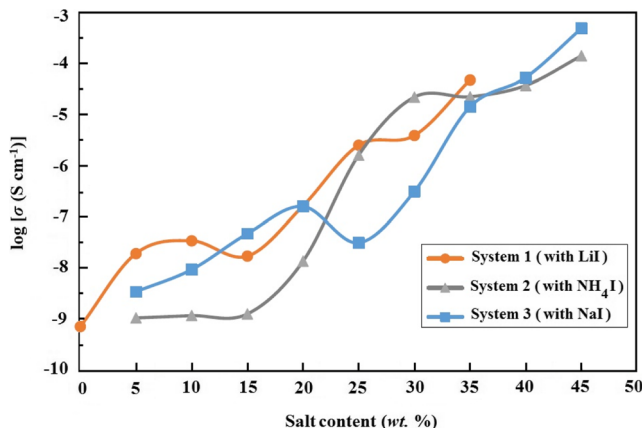


Fig. 1 Ionic conductivity of three polymer electrolyte systems

Table 2 Bulk resistance of three polymer electrolyte systems

Designation			Bulk resistance, R_b (Ω)		
S1	S2	S3	S1	S2	S3
RS-0	–	–	4.0×10^6	–	–
RS-1	RN-1	RNa-1	3.14×10^5	3.87×10^6	8.79×10^5
RS-2	RN-2	RNa-2	9.57×10^4	3.15×10^6	2.49×10^5
RS-3	RN-3	RNa-3	2.26×10^5	2.89×10^6	6.70×10^4
RS-4	RN-4	RNa-4	1.43×10^4	2.36×10^5	1.80×10^4
RS-5	RN-5	RNa-5	1.03×10^3	2.16×10^3	1.04×10^5
RS-6	RN-6	RNa-6	9.81×10^2	1.48×10^2	9.02×10^3
RS-7	RN-7	RNa-7	96.0	1.30×10^2	2.25×10^2
RS-8	RN-8	RNa-8	–	70.3	52.1
RS-9	RN-9	RNa-9	–	17.3	11.4

$$\sigma = \frac{2}{3} \left[\frac{(Ze)^2}{kTm} \right] nE_a\tau_0 \exp\left(\frac{-E_a}{kT}\right) \tag{1}$$

where Ze denotes the charge carried by an ion belonging to the conducting species, in which Z is the valency of ion, k is the Boltzmann constant, m is the mass of ionic carrier, n is the number density of mobile ions, and τ_0 is the free ion lifetime. In Eq. (1), the term m as mass of ionic carrier shows that, when mass increases, the ionic conductivity will increase as well. The molar mass of NaI is ~ 22.99 g/mol where the molar mass of LiI and NH_4I are ~ 6.941 and ~ 18.000 g/mol, respectively [$m(\text{NaI}) > m(\text{NH}_4\text{I}) > m(\text{LiI})$].

Figure 2 demonstrates the Cole–Cole plot for (a) RS-7, (b) RN-9, and (c) RNa-9 as the highest achieved ionic conductivities in all three systems. In the graph, the equivalent circuit for the RNa-9 SPE is represented with the C_e as double-layer capacitance, C for geometric capacitance, and R as resistance with equivalent values of 1 μF , 0.1 μF , and 100 Ω , respectively.

Temperature-dependent ionic conductivity

Figure 3 illustrates temperature-dependent results for the polymer electrolytes with the highest ionic conductivity in each system namely RS-7, RN-9, and RNa-9. The regressions ($R^2 \sim 0.99$) show that each system follows Arrhenius thermal-activated model according to the below equation

$$\sigma = \sigma_0 \exp\left[\frac{-E_a}{kT}\right] \tag{2}$$

where σ_0 is the pre-exponential factor, E_a is the activation energy, and k is the Boltzmann constant. The activation

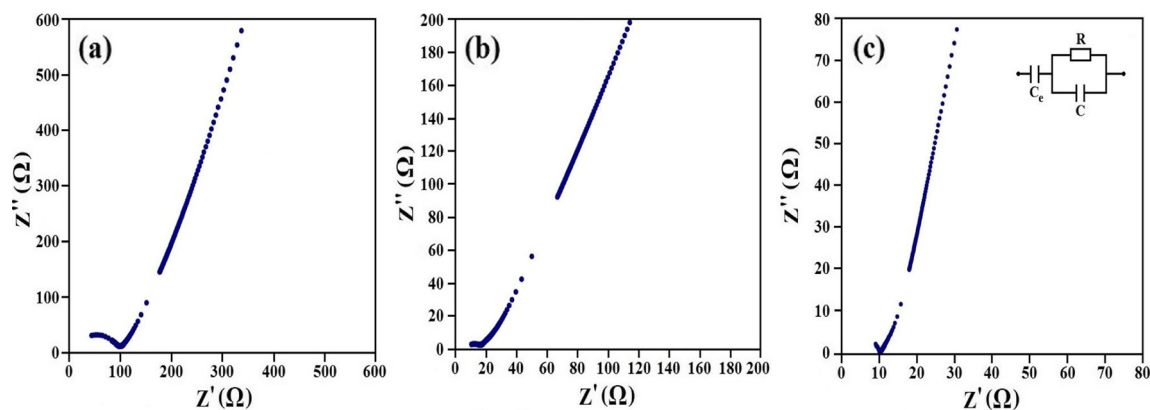


Fig. 2 Cole–Cole plot of RNa-9 with equivalent circuit

energies calculated for RS-7, RN-9, and RNa-9 are 0.41, 0.16, and 0.11 eV, respectively. The results show that activation energy decreases with an increase in ionic conductivity, and the lowest activation energy is for sample RNa-9 as highest achieved ionic conductivity.

Fourier transform infrared

The FTIR spectra for system S2 (with NH_4I) are represented in Fig. 4 at different wavenumbers between 4000 and 400 cm^{-1} . The band assignments for polymer electrolyte contents according to the literature [20–22] are depicted in Table 3. Results show that the peaks in pure rice starch (RS-0) shifts to another frequency after addition of ammonium iodide salt. The peak in 3310 cm^{-1} for RS-0 shifts to lower frequencies of 3222 , 3197 , and 3197 cm^{-1} in RN-7, RN-8, and RN-9, respectively, after incorporation of NH_4I . For the peak at 997 cm^{-1} in RS-0, the frequency shifts to higher frequencies of 1012 , 1013 , and 1015 cm^{-1} due to NH_4I spectra. The shifts express that the complexation between polymer (RS-0) and salt (NH_4I) has occurred. The complexation between RS-0 and LiI has been discussed in the previous work [17].

The FTIR spectra for system S3 (with NaI) are illustrated in Fig. 5. Similarly, the spectra show complexation between RS-

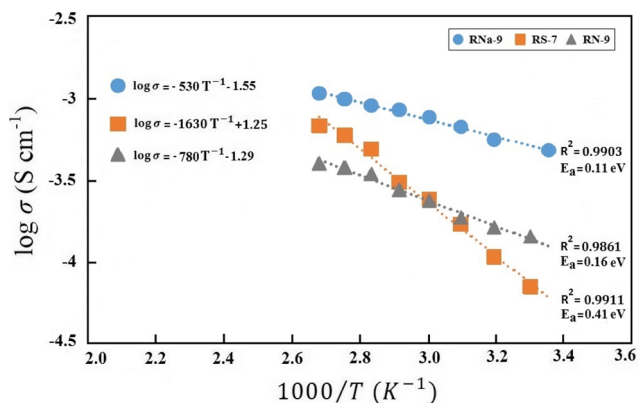


Fig. 3 Temperature-dependence ionic conductivity of RS-7, RN-9, and RNa-9

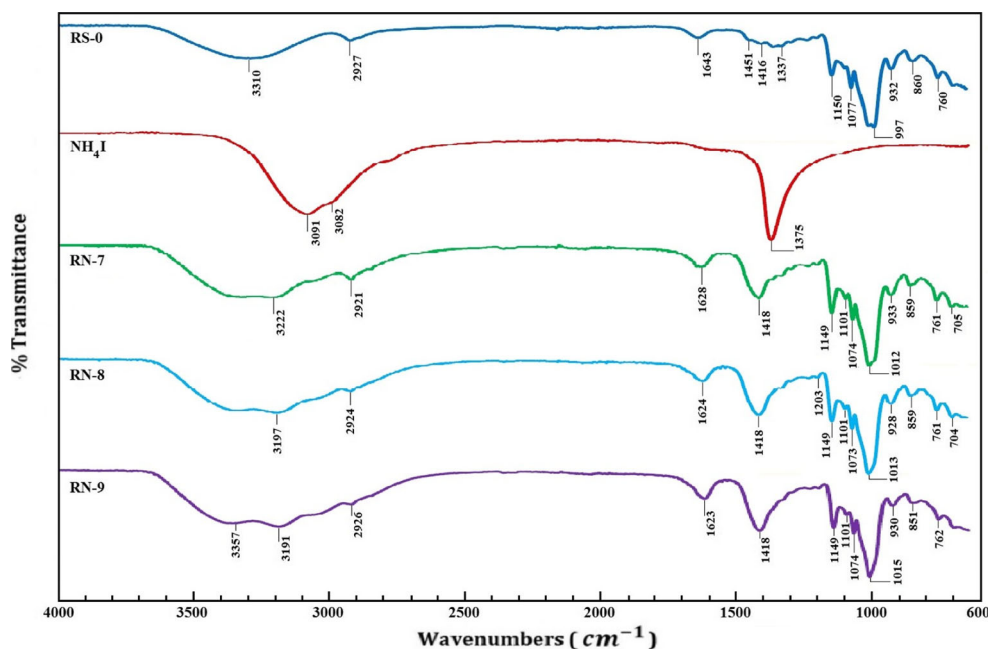
0 and NaI salt. The peak at 3310 cm^{-1} for RS-0 shifts to higher frequencies of 3356 , 3354 , and 3373 cm^{-1} in RNa-7, RNa-8, and RNa-9, respectively, after addition of NaI salt. The peak in 1643 cm^{-1} for RS-0 shifts to lower frequencies of 1635 , 1635 , and 1624 cm^{-1} in RNa-7, RNa-8, and RNa-9, respectively. Thus, the FTIR spectra in all three systems prove complexation between polymer and iodide salts. Furthermore, the shifting of frequency to lower in NH_4I -based system and to higher in NaI-based system may be due to more or less accumulation and aggregation of NaI salt [23, 24].

X-ray diffraction

The XRD patterns of system S2 with ammonium iodide are represented in Fig. 6. The graph shows XRD patterns of (a) RN-7, (b) RN-8, (c) RN-9, (d) RS-0 (pure rice starch), and (e) NH_4I . The ammonium iodide patterns show crystalline characteristics with sharp peaks at $2\theta=21$ and 24° , with other peaks at $2\theta=35$, 41 , and 43° . Pure rice starch pattern in Fig. 6d exhibits amorphous characteristics with a small peak at $2\theta=19^\circ$ and a broad hunch at $2\theta=17$ – 22° . After incorporation of NH_4I salt the peaks in RS-0, 2θ shifts to higher range of 19 – 25° for RN-7, 18 – 25° for RN-8, and 19 – 25° for RN-9. The shifts confirm complexation of ammonium iodide salt with pure rice starch. The graph shows elimination of peaks in ammonium iodide. The results further confirm complexation of pure rice starch.

The XRD patterns of system S3 with sodium iodide (NaI) are demonstrated in Fig. 7 for (a) RNa-7, (b) RNa-8, (c) RNa-9, (d) pure rice starch, and (e) NaI. Figure 6e shows very sharp crystalline peak at $2\theta=22.1$ and 46.7° , and several other crystalline peaks at $2\theta=15.5$, 18.3 , and 42.5° for sodium iodide salt denoting crystalline characteristic of NaI salt. The peaks in pure rice starch shifts to higher value after addition of NaI to the range of 19 – 24° in RNa-7, 19 – 25° in RNa-8, and 18 – 25° in RNa-9. The results show broadening of pure rice starch change after addition of sodium iodide salt. These results further confirm complexation of pure rice starch and NaI salt. In addition, complexation between pure rice starch and lithium iodide (LiI)

Fig. 4 FTIR spectra of RS-0, NH₄I, RN-7, RN-8, and RN-9 polymer electrolytes



has been confirmed in our previous work [17]. The system S3 shows more broadening, which is the result of more amorphousness of system S3 according to the XRD patterns.

Table 3 Band assignments and wavenumbers for polymer electrolytes

Wavenumbers (cm ⁻¹)				Band assignments
RS	NH ₄ I	RS+NH ₄ I	RS+NaI	
3310		3357, 3191	3373	O–H stretching (broad) N–H stretch, alkynes
	3091, 3082			
2927		2926	2931	C–H ₂ deformation (m)–(CH ₂)
	2798			H–C=O:C–H stretch, aldehydes
1643		1623	1624	H ₂ O in amorphous regions of starch
	1616			C–C stretch(in ring), aromatic
1451				C–H bending (v)–(CH ₂)
	1375			NH ₄ asymmetric H–N–H deformation
1337			1363	C–O–H bending, C–H twisting (CH ₂)
1150		1149	1150	C–O stretching (s)
1077		1074	1073	C–O–H bending (s)
997		1015	1015	C–H bending (v)
932		930	931	Skeletal mode vibrations of α-1,4-glycosidic linkages (C–O–C)
860		851	845	C–H deformation
760		762	758	C–C stretching (v)

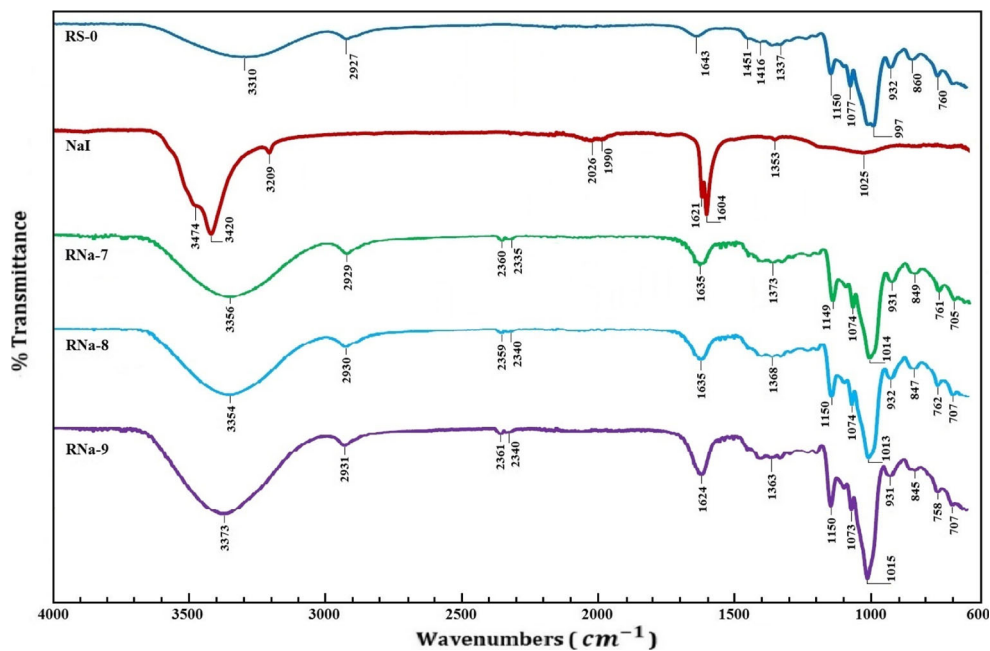
RS rice starch, (s) strong, (m) medium, (v) variable

TGA and DSC

Figure 8 shows TGA graph of system S2 for pure rice starch (RS-0) and selected samples of RN-7, RN-8, and RN-9. The graph shows that the decomposition temperature (*T*_{dc}) decrease dramatically from 292 °C (pure rice starch) to 187, 185, and 184 °C for RN-7, RN-8, and RN-9, respectively, after addition of NH₄I salt with one-step decomposition. Figure 9 shows TGA graph of system S3 for pure rice starch (RS-0), RN_a-7, RN_a-8, and RN_a-9. The graph shows decrease in *T*_{dc} to 245, 243, and 242 °C for RN_a-7, RN_a-8, and RN_a-9, respectively, after addition of NaI salt. Furthermore, *T*_{dc} decreases in system S1 upon addition of LiI salt [17]. The reason for the decrease in *T*_{dc} after addition of iodide salt can be due to complexation of rice starch and iodide salt, which results in more segmental flexibility of polymeric network, which can reduce the decomposition temperature of polymer electrolyte.

The systems are further analyzed for thermal study using DSC. The glass transition temperature (*T*_g) for pure rice starch is ~76 °C. After addition of salt, glass transition temperature suddenly decreases. In system 1, *T*_g values for samples of RS-5, RS-6, and RS-7 are –23, –22, and –12 °C, respectively. In system 2, *T*_g values for samples of RN-7, RN-8, and RN-9 are –40, –39, and –38 °C, respectively. Consequently, in system 3, *T*_g for RN_a-7, RN_a-8, and RN_a-9 are –43, –43, and –42 °C, respectively. The *T*_g shifts by addition of LiI, NH₄I, and NaI, but the shift in NH₄I- and NaI-based systems are larger than that in LiI-based system. The reason can be expressed by molecular mass of iodide salts, where the molecular mass of LiI is 133.85 g/mol, for NH₄I is 144.94 g/mol, and for NaI is

Fig. 5 FTIR spectra of RS-0, NaI, RNa-7, RNa-8, and RNa-9 polymer electrolytes



149.89 g/mol [$M_n(\text{NaI}) > M_n(\text{NH}_4\text{I}) > M_n(\text{LiI})$]. It can be noted that the molar mass of sodium iodide and ammonium iodide are very close to each other, but for LiI, there is

a significant difference. Consequently, this can be explained by the Flory–Fox equation as below equation [25, 26]

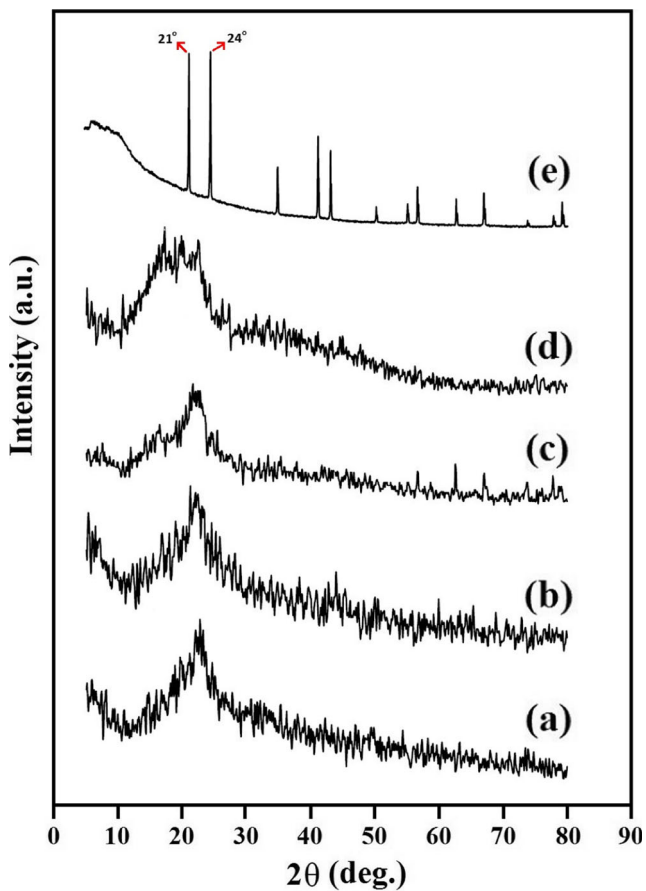


Fig. 6 XRD patterns of polymer electrolytes in system 2 for **a** RN-7, **b** RN-8, **c** RN-9, **d** pure rice starch (RS-0), and **e** NH_4I

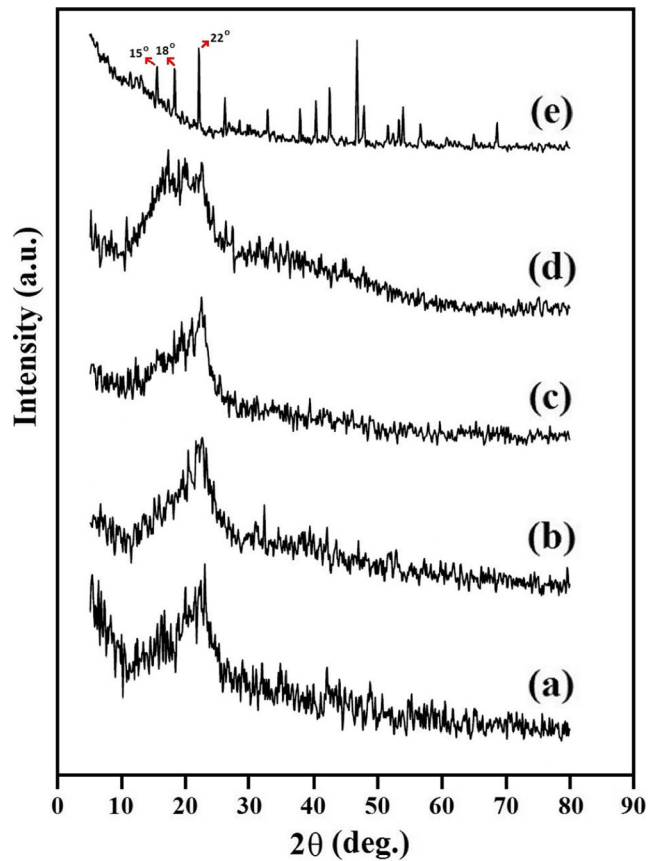


Fig. 7 XRD patterns of polymer electrolytes in system 3 for **a** RNa-7, **b** RNa-8, **c** RNa-9, **d** pure rice starch (RS-0), and **e** NaI

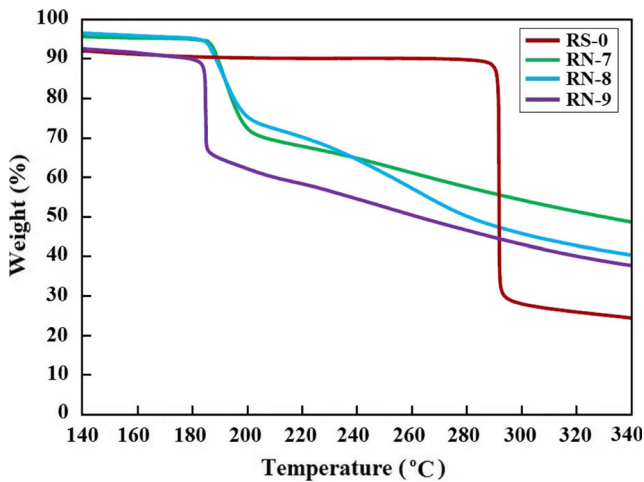


Fig. 8 TGA thermograms for RS-0, RN-7, RN-8, and RN-9 in system 2

$$T_g = T_{g,\infty} - \frac{K}{M_n} \tag{3}$$

where $T_{g,\infty}$ is the maximum glass transition temperature by theoretical infinite molecular mass, K is the an empirical parameter related to the free volume of sample, and M_n is molecular mass. Thus, the Flory–Fox equation confirms that the LiI with lower molecular mass is predicted to have lower glass transition temperature. The results show that T_g shifts to higher temperatures with increasing iodide salt. This is due to existing complexation upon addition of salt with flexibility of polymer chains [27]. Thermal study on polymer electrolytes further confirm complexation of pure rice starch with iodide salt and results in changing thermal properties after addition of iodide salts. The thermal parameters are depicted in Table 4.

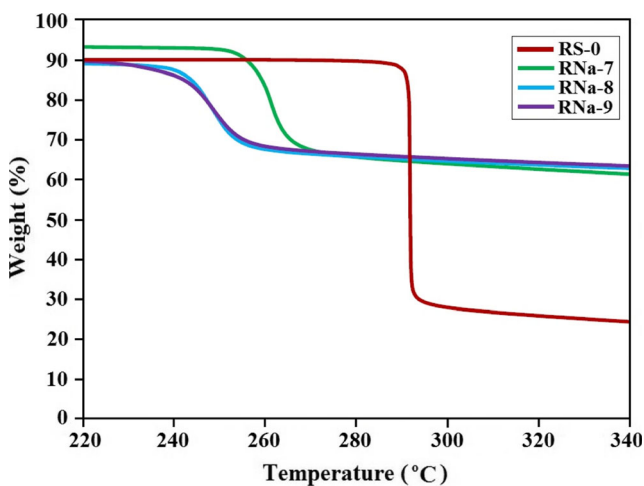


Fig. 9 TGA thermograms for RS-0, RN-7, RN-8, and RN-9 in system 3

Table 4 TGA and DSC data for three polymer electrolyte systems

Samples		Decomposition temperature (T_{dc}) (°C)	Decomposition steps	Glass transition temperature (T_g) (°C)
S1	RS-0	292	Single step	76
	RS-5	245	Single step	−23
	RS-6	230	Single step	−22
	RS-7	224	Single step	−12
S2	RN-7	187	Single step	−40
	RN-8	185	Single step	−39
	RN-9	184	Single step	−38
S3	RNa-7	245	Single step	−43
	RNa-8	243	Single step	−43
	RNa-9	242	Single step	−42

Dye-sensitized solar cell

The dye-sensitized solar cell (DSSC) was fabricated using RNa-9 as the highest ionic conductivity between all systems. The J – V characteristic curve of fabricated dye-sensitized solar cell using RNa-9 with N719 dye is illustrated in Fig. 10. The fill factor was calculated as

$$ff = \frac{J_{max} V_{max}}{J_{sc} V_{oc}} \tag{4}$$

where J_{max} (mA cm^{-2}) and V_{max} (V) are the current density and voltage at maximum power output, and J_{sc} (mA cm^{-2}) and V_{oc} (V) are short-circuit current density and open-circuit voltage. The efficiency (η) was calculated using

$$\eta = \frac{J_{max} \cdot V_{max} \cdot ff}{P_{in}} \tag{5}$$

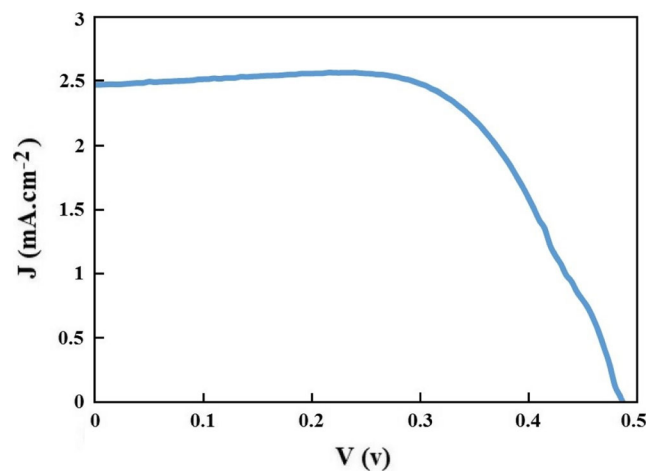


Fig. 10 Photocurrent density versus cell potential (J – V) for DSSC fabricated using RNa-9

where P_{in} is incident light power. The DSSC cell was analyzed under Sun simulator with light power of 100 mW/cm^2 . DSSC parameters of J_{sc} (mA cm^{-2}), V_{oc} (V), ff , and η (%) of the RNa-9 are 2.40, 0.485, 0.67, and 0.78, respectively. Between polymer-electrolyte-based DSSCs using biodegradable polymers, Singh et al. [28] achieved 0.54 % with composition of agarose/KI polymer-electrolyte-based DSSC. Consequently, Singh et al. [1] achieved efficiency of 0.63 % with composition of Arrowroot starch/KI polymer-electrolyte-based DSSC. The results obtained in this work show enhanced energy conversion efficiency (0.78 %) compared with several other works performed recently using biodegradable polymers.

Conclusion

The polymer electrolytes were prepared using solution cast technique. The samples were prepared in three different systems using lithium iodide, ammonium iodide, and sodium iodide. The highest ionic conductivity of $4.79 \times 10^{-4} \text{ S/cm}$ was achieved in system 3 upon introducing 45 wt% of sodium iodide salt with designation of RNa-9. Temperature-dependent ionic conductivity study confirmed that all polymer electrolytes follow Arrhenius thermal-activated model. Structural and thermal analyses confirmed complexation between pure rice starch and salt. Dye-sensitized solar cell was fabricated using RNa-9 as environmental friendly polymer electrolyte and analyzed with Sun simulator in 100 mW/cm^2 . The J - V graph showed energy conversion efficiency of 0.78 %. This work can be further studied to enhance the ionic conductivity and efficiency of DSSC with incorporation of ionic liquids as future work.

Acknowledgments M. H. Khanmirzaei acknowledges the University of Malaya Bright Sparks Scheme (SBSUM) for the financial support (BSP 221(3)-12). This work was supported by the University of Malaya Research Grant (UMRG Program: RP025A-14AFR) and Fundamental Research Grant Scheme (FRGS: FP024-2013A)

References

- Singh R, Bhattacharya B, Rhee HW, Singh PK (2014) New biodegradable polymer electrolyte for dye sensitized solar cell. *Int J Electrochem Sci* 9(5):2620–2630
- Liang GJ, Zhong ZC, Xu J, Zhang ZC, Chen MH, Li ZF, He P, Hou QF (2012) Quasi-solid state dye-sensitized solar cells based on the novel crosslinked polymer electrolyte. *Acta Phys-Chim Sin* 28(12):2852–2860
- Polo Fonseca C, Neves S (2006) Electrochemical properties of a biodegradable polymer electrolyte applied to a rechargeable lithium battery. *J Power Sources* 159(1):712–716
- Johari NA, Kudin TIT, Ali AMM, Winie T, Yahya MZA (2009) Studies on cellulose acetate-based gel polymer electrolytes for proton batteries. *Mater Res Innov* 13(3):232–234
- Rao M, Li X, Liao Y, Li X, Li W (2015) Preparation and performance of a composite polyimide/poly(vinylidene fluoride-co-hexafluoropropylene)/nano- Al_2O_3 polymer electrolyte for lithium-sulfur cell. *Ionics*:1–7
- Polu A, Kumar R, Rhee H-W (2015) Magnesium ion conducting solid polymer blend electrolyte based on biodegradable polymers and application in solid-state batteries. *Ionics* 21(1):125–132
- Sudhakar YN, Selvakumar M (2012) Lithium perchlorate doped plasticized chitosan and starch blend as biodegradable polymer electrolyte for supercapacitors. *Electrochim Acta* 78:398–405
- Sudhakar YN, Selvakumar M, Bhat DK (2013) LiClO_4 -doped plasticized chitosan and poly(ethylene glycol) blend as biodegradable polymer electrolyte for supercapacitors. *Ionics* 19(2):277–285
- Hashmi SA, Latham RJ, Linford RG, Schlindwein WS (1997) Polymer electrolyte based solid state redox supercapacitors with poly(3-methyl thiophene) and polypyrrole conducting polymer electrodes. *Ionics* 3(3–4):177–183
- Ma J, Sahai Y (2013) Chitosan biopolymer for fuel cell applications. *Carbohydr Polym* 92(2):955–975
- Rahman NFA, Shyuan LK, Mohamad A, Kadhum AAH (2013) Review on biopolymer membranes for fuel cell applications. In: Tang X, Chen X, Dong Y, Wei X, Yang Q (eds) *Advances in energy science and technology*, Pts 1–4, vol 291–294. Applied mechanics and materials. Trans Tech Publications Ltd, Stafa-Zurich, pp 614–617
- Zhou D, Zhou R, Chen CX, Yee WA, Kong JH, Ding GQ, Lu XH (2013) Non-volatile polymer electrolyte based on poly(propylene carbonate), ionic liquid, and lithium perchlorate for electrochromic devices. *J Phys Chem B* 117(25):7783–7789
- Kumar M, Tiwari T, Srivastava N (2012) Electrical transport behaviour of bio-polymer electrolyte system: potato starch plus ammonium iodide. *Carbohydr Polym* 88(1):54–60
- Marcondes R, D'Agostini PS, Ferreira J, Giroto EM, Pawlicka A, Dragunski DC (2010) Amylopectin-rich starch plasticized with glycerol for polymer electrolyte application. *Solid State Ion* 181(13–14):586–591
- Teoh KH, Lim CS, Ramesh S (2014) Lithium ion conduction in corn starch based solid polymer electrolytes. *Measurement* 48:87–95
- Zhang CQ, Zhu LJ, Shao K, Gu MH, Liu QQ (2013) Toward underlying reasons for rice starches having low viscosity and high amylose: physicochemical and structural characteristics. *J Sci Food Agric* 93(7):1543–1551
- Khanmirzaei MH, Ramesh S (2013) Ionic transport and FTIR properties of lithium iodide doped biodegradable rice starch based polymer electrolytes. *Int J Electrochem Sci* 8(7):9977–9991
- Singh R, Baghel J, Shukla S, Bhattacharya B, Rhee H-W, Singh PK (2014) Detailed electrical measurements on sago starch biopolymer solid electrolyte. *Phase Transit* 87(12):1237–1245
- Rice MJ, Roth WL (1972) Ionic transport in super ionic conductors: a theoretical model. *J Solid State Chem* 4(2):294–310
- Kizil R, Irudayaraj J, Seetharaman K (2002) Characterization of irradiated starches by using FT-Raman and FTIR spectroscopy. *J Agric Food Chem* 50(14):3912–3918
- Pretsch E, Bühlmann P, Badertscher M (2009) *Structure determination of organic compounds: tables of spectral data*. 4th, rev. and enl. edn. Springer, Berlin
- Singh VK, Annu A, Singh U, Singh P, Pandey SP, Bhattacharya B, Singh PK (2013) Dye sensitized solar cell based on poly(vinyl alcohol) doped with ammonium iodide solid polymer electrolyte. *J Optoelectron Adv Mater* 15(9–10):927–931

23. Liang G, Zhong Z, Qu S, Wang S, Liu K, Wang J, Xu J (2013) Novel in situ crosslinked polymer electrolyte for solid-state dye-sensitized solar cells. *J Mater Sci* 48(18):6377–6385
24. Tara-Lunga-Mihali M, Plesu N, Macarie L, Iliescu S, Ilia G (2014) Polyaniline composite designed for solid polymer electrolyte. *Pure Appl Chem* 86(11):1853–1860
25. Fox TG, Flory PJ (1950) Second-order transition temperatures and related properties of polystyrene. I: influence of molecular weight. *J Appl Phys* 21(6):581–591
26. Bueche F (1956) Derivation of the WLF equation for the mobility of molecules in molten glasses. *J Chem Phys* 24(2):418–419
27. Tominaga Y, Asai S, Sumita M, Panero S, Scrosati B (2005) A novel composite polymer electrolyte: effect of mesoporous SiO₂ on ionic conduction in poly(ethylene oxide)–LiCF₃SO₃ complex. *J Power Sources* 146(1–2):402–406
28. Singh R, Jadhav NA, Majumder S, Bhattacharya B, Singh PK (2013) Novel biopolymer gel electrolyte for dye-sensitized solar cell application. *Carbohydr Polym* 91(2):682–685